



**HAL**  
open science

## Experimental Determination of $\alpha$ Widths of Ne21 Levels in the Region of Astrophysical Interest: New O17+ $\alpha$ Reaction Rates and Impact on the Weak s Process

F Hammache, P Adsley, L Lamia, D.S Harrouz, N de Séréville, B Bastin, A Choplin, T Faestermann, C Fougères, R Hertenberger, et al.

### ► To cite this version:

F Hammache, P Adsley, L Lamia, D.S Harrouz, N de Séréville, et al.. Experimental Determination of  $\alpha$  Widths of Ne21 Levels in the Region of Astrophysical Interest: New O17+ $\alpha$  Reaction Rates and Impact on the Weak s Process. *Physical Review Letters*, 2024, 132 (18), pp.182701. 10.1103/PhysRevLett.132.182701 . hal-04566078

**HAL Id: hal-04566078**

**<https://hal.science/hal-04566078v1>**

Submitted on 29 Oct 2024

**HAL** is a multi-disciplinary open access archive for the deposit and dissemination of scientific research documents, whether they are published or not. The documents may come from teaching and research institutions in France or abroad, or from public or private research centers.

L'archive ouverte pluridisciplinaire **HAL**, est destinée au dépôt et à la diffusion de documents scientifiques de niveau recherche, publiés ou non, émanant des établissements d'enseignement et de recherche français ou étrangers, des laboratoires publics ou privés.

# First experimental determination of $\alpha$ widths of $^{21}\text{Ne}$ levels in the region of astrophysical interest: new $^{17}\text{O}+\alpha$ reaction rates and impact on the weak s-process

F. Hammache,<sup>1,\*</sup> P. Adsley,<sup>2,3,†</sup> L. Lamia,<sup>4,5,6</sup> D. S. Harrouz,<sup>1</sup> N. de Séréville,<sup>1</sup> B. Bastin,<sup>7</sup> A. Choplin,<sup>8</sup> T. Faestermann,<sup>9</sup> C. Fougères,<sup>7</sup> R. Hertenbergger,<sup>10</sup> R. Hirschi,<sup>11,12</sup> M. La Cognata,<sup>4</sup> A. Meyer,<sup>1</sup> S. Palmerini,<sup>13,14</sup> R. G. Pizzone,<sup>4</sup> F. de Oliveira Santos,<sup>7</sup> S. Romano,<sup>4,5,6</sup> A. Tumino,<sup>4,15</sup> and H.-F. Wirth<sup>10</sup>

<sup>1</sup> *Université Paris-Saclay, CNRS/IN2P3, IJCLab, 91405 Orsay, France*

<sup>2</sup> *School of Physics, University of the Witwatersrand, Johannesburg 2050, South Africa*

<sup>3</sup> *Themba Laboratory for Accelerator Based Sciences, Somerset West 7129, South Africa*

<sup>4</sup> *Laboratori Nazionali del Sud - Istituto Nazionale di Fisica Nucleare, Via Santa Sofia 62, 95123 Catania, Italy*

<sup>5</sup> *Dipartimento di Fisica e Astronomia E. Majorana, Univ. di Catania, Catania, Italy*

<sup>6</sup> *Centro Siciliano di Fisica Nucleare e Struttura della Materia-CSFNSM, Catania, Italy*

<sup>7</sup> *Grand Accélérateur National d'Ions Lourds (GANIL),*

*CEA/DRF-CNRS/IN2P3, Bd. Henri Becquerel, 14076 Caen, France*

<sup>8</sup> *Institut d'Astronomie et d'Astrophysique, Université libre de Bruxelles, CP 225, B-1050 Brussels, Belgium*

<sup>9</sup> *Physik Department E12, Technische Universität München, D-85748 Garching, Germany*

<sup>10</sup> *Fakultät für Physik, Ludwig-Maximilians-Universität München, D-85748 Garching, Germany*

<sup>11</sup> *Astrophysics Research Center, Keele University, Keele, Staffordshire ST5 5BG, UK*

<sup>12</sup> *Kawli IPMU (WPI), University of Tokyo, 5-1-5 Kashiwanoha, Kashiwa 277-8583, Japan*

<sup>13</sup> *Dipartimento di Fisica e Geologia, Università degli Studi di Perugia, Perugia, Italy*

<sup>14</sup> *Istituto Nazionale di Fisica Nucleare, Sezione di Perugia, Perugia, Italy*

<sup>15</sup> *Facoltà di Ingegneria e Architettura, Università degli Studi di Enna, Italy*

(Dated: October 29, 2024)

The efficiency of the weak s-process in low-metallicity rotating massive stars depends strongly on the rates of the competing  $^{17}\text{O}(\alpha, n)^{20}\text{Ne}$  and  $^{17}\text{O}(\alpha, \gamma)^{21}\text{Ne}$  reactions which determine the potency of the  $^{16}\text{O}$  neutron poison. Their reaction rates are poorly known in the astrophysical energy range of interest for core helium burning in massive stars because of the lack of spectroscopic information (partial widths, spin-parities) for the relevant states in the compound nucleus  $^{21}\text{Ne}$ . In this Letter, we report on the first experimental determination of the  $\alpha$ -particle spectroscopic factors and partial widths of these states using the  $^{17}\text{O}({}^7\text{Li}, t)^{21}\text{Ne}$   $\alpha$ -transfer reaction. With these the  $^{17}\text{O}(\alpha, n)^{20}\text{Ne}$  and  $^{17}\text{O}(\alpha, \gamma)^{21}\text{Ne}$  reaction rates were evaluated with uncertainties reduced by a factor more than three with respect to previous evaluations and the present  $^{17}\text{O}(\alpha, n)^{20}\text{Ne}$  reaction rate is more than twenty times larger. The present  $(\alpha, n)/(\alpha, \gamma)$  rate ratio favours neutron recycling and suggests an enhancement of the weak s-process in the Zr-Nd region by more than 1.5 dex in metal-poor rotating massive stars.

Nearly half of the abundance of heavy elements originates from the s-process, a sequence of slow neutron-capture reactions, occurring in two major astrophysical sites: asymptotic giant branch stars and massive stars. During core-He burning in massive stars, the  $^{22}\text{Ne}(\alpha, n)^{25}\text{Mg}$  reaction is the main neutron source for the weak s-process component, producing elements between iron and strontium. Models of rotating low-metallicity massive stars [1, 2] show a potential large production of heavier s-elements between strontium and barium during the helium core burning phase.

The efficiency of the s-process in these stars depends on two competing thermonuclear reactions:  $^{17}\text{O}(\alpha, n)^{20}\text{Ne}$  and  $^{17}\text{O}(\alpha, \gamma)^{21}\text{Ne}$  [1–3]. Their ratio determines the poisoning effect of  $^{16}\text{O}$  consuming neutrons released by the  $^{22}\text{Ne}(\alpha, n)^{25}\text{Mg}$  reaction by  $^{16}\text{O}(n, \gamma)^{17}\text{O}$ . The neutrons may be recycled by  $^{17}\text{O}(\alpha, n)^{20}\text{Ne}$  or lost for good through  $^{17}\text{O}(\alpha, \gamma)^{21}\text{Ne}$ . At He-core burning temperatures of 0.2–0.3 GK the  $^{17}\text{O}(\alpha, n)^{20}\text{Ne}$  and  $^{17}\text{O}(\alpha, \gamma)^{21}\text{Ne}$  reactions are dominated by resonances of energy  $E_r^{c.m.} \sim 0.28\text{--}0.65$  MeV corresponding to excited states between  $E_x = 7.620$  and  $8.00$  MeV ( $S_\alpha = 7347.93(4)$  keV [4]) in

$^{21}\text{Ne}$ . For these excited states, the spectroscopic data ( $\alpha$ -particle, neutron and  $\gamma$ -ray partial widths and spin-parities) are poorly known or unknown resulting in large uncertainties in the  $(\alpha, n)$  and  $(\alpha, \gamma)$  reaction rates [5].

To investigate the neutron recycling efficiency and reduce the large uncertainties on both reaction rates, we report here on the pioneering experimental determination of the  $\alpha$ -widths of the resonance states of interest in  $^{21}\text{Ne}$  through the measurement of  $\alpha$ -spectroscopic factors. These were determined from the  $\alpha$ -transfer reaction  $^{17}\text{O}({}^7\text{Li}, t)^{21}\text{Ne}$  performed at MLL-Munich, using the high energy resolution Q3D magnetic spectrograph [6].

A 28-MeV  ${}^7\text{Li}^{3+}$  beam was delivered by the 14-MV Tandem of MLL-Munich with typical intensity around 100 enA measured with a suppressed Faraday cup at  $0^\circ$  downstream from the target. An enriched  $40(1)\mu\text{g}/\text{cm}^2$   $\text{W}^{17}\text{O}_3$  target with 35% enrichment in  $^{17}\text{O}$  on a  $34(1)\mu\text{g}/\text{cm}^2$  C backing was used. A target of natural  $39(1)\mu\text{g}/\text{cm}^2$   $\text{WO}_3$  on  $35(1)\mu\text{g}/\text{cm}^2$  C was used for calibration and background evaluation. The absolute amount of  $^{17}\text{O}$ ,  $^{16}\text{O}$ ,  $^{18}\text{O}$  and  $^{12}\text{C}$  present in the enriched

and natural targets was deduced from Rutherford Back Scattering at JANNus/SCALP [7]. Trace contamination of  $^{14}\text{N}$  was observed in both enriched and natural targets.

The reaction products were momentum analyzed in the Q3D with solid angle between 6 to 12.4 msr depending on the measured angle. Tritons were unambiguously identified at the focal plane [8] using two proportional gas-counters providing the focal-plane position and energy losses of the detected particles backed by a plastic scintillator measuring the residual energy.

Tritons were detected at nine laboratory angles ( $6^\circ$  to  $36^\circ$ ), covering astrophysically relevant excitation energies from 7.1 to 8.25 MeV. The energy resolution was 30 keV to 70 keV, worsening with increasing angle. Triton position spectra measured at  $9^\circ$  and  $28^\circ$  with the enriched  $\text{W}^{17}\text{O}_3$  target are displayed in Fig. 1.

All known states of  $^{21}\text{Ne}$  in the region of interest ( $E_x = 7.420 - 8.155$  MeV) are observed except the  $7.469$ - ( $J^\pi = 1/2^-, 3/2^-$ ) and the  $8.009$ -MeV ( $J^\pi = 1/2^-$ ) states which are not or very weakly populated. Some states could not be observed at all angles because of the presence of the  $E_x = 6.92$ - and  $7.12$ -MeV contaminant states in  $^{16}\text{O}$ .

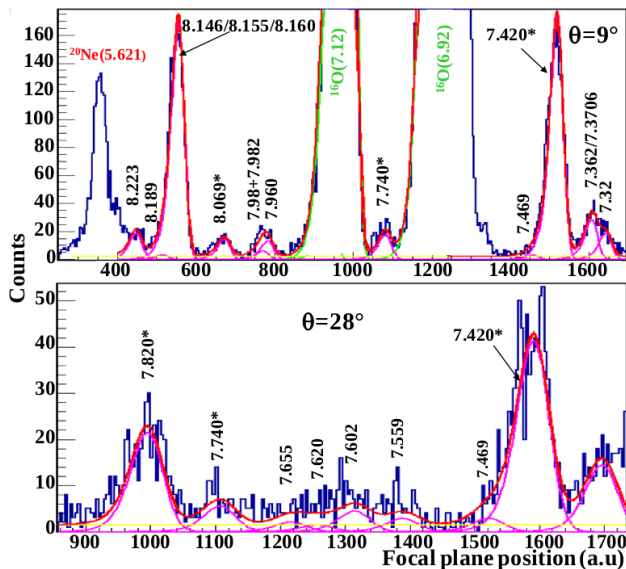


FIG. 1. (Color online) Triton position spectra at spectrograph angles of  $9^\circ$  (top panel) and  $28^\circ$  (bottom panel).  $^{21}\text{Ne}$  excited states are labeled in black while states labeled in red and green belong to  $^{20}\text{Ne}$  and  $^{16}\text{O}$  contaminants, respectively. The best fit is shown as a red line, while the individual contributions are in pink ( $^{21}\text{Ne}$ ) and green ( $^{16}\text{O}$ ). The yellow flat curve corresponds to the background.

The triton spectra were fitted using a sum of exponentially modified Gaussian functions accounting for the Q3D response. At each angle a common width and exponential factor from the isolated  $7.420$ -MeV state were used for all  $^{21}\text{Ne}$  states. Given the energy resolution,

the triplet of states at  $E_x = 8.146, 8.155$  and  $8.160$  MeV was treated as a single state as was the  $E_x = 7.980$ - and  $7.982$ -MeV doublet. The  $^{16}\text{O}$  contaminant peaks were either excluded from the fit or included when close to the states of interest.

The  $\chi^2$  minimization provides the peak yields and uncertainty which varies by state and angle from 3% for the strongest at small angles to nearly 77% for the weakest at larger angles due to degraded energy resolution and smaller differential cross sections. The contamination due to  $^{16}\text{O}(^7\text{Li},t)^{20}\text{Ne}$  and  $^{14}\text{N}(^7\text{Li},t)^{18}\text{F}$  reactions was evaluated with the natural  $\text{WO}_3$  target and subtracted from the  $^{21}\text{Ne}$  peak yields after charge and target composition normalisation. The level of  $^{22}\text{Ne}$  contamination due  $^{18}\text{O}(^7\text{Li},t)^{22}\text{Ne}$  reaction was evaluated to be below or at most at background level [9].

The measured  $^{17}\text{O}(^7\text{Li},t)^{21}\text{Ne}$  differential cross sections are displayed in Fig. 2 including the  $E_x = 7.655$ -,  $7.74$ -,  $7.82$ - and  $7.96$ - MeV states of interest. Those of the  $E_x = 7.559$ -,  $7.602$ - and  $7.620$ - states are displayed in [9]. The uncertainties of the cross sections arise from the quadratic sum of the peak yield uncertainty determined at each measured angle, the number of target atoms, the solid angle and the total number of incoming  $^7\text{Li}$  particles.

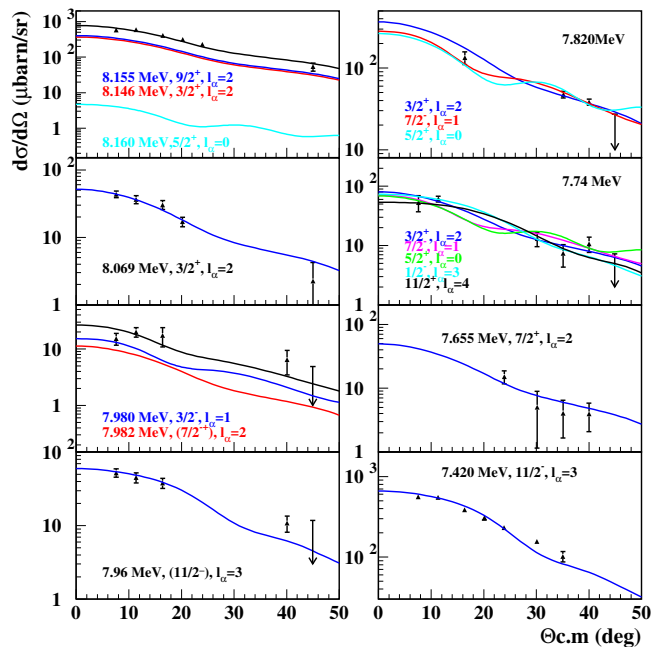


FIG. 2. (Color online) Experimental differential cross-sections of the  $^{17}\text{O}(^7\text{Li},t)^{21}\text{Ne}$  reaction obtained at  $E_{^7\text{Li}} = 28$  MeV for different populated states in  $^{21}\text{Ne}$  together with DWBA calculations normalized to the data. See text for details.

Theoretical cross sections were obtained from FRESKO finite-range DWBA calculations [11]. The  $\alpha$ -spectroscopic factors  $C^2S_\alpha$  were obtained by normaliza-

tion of the theoretical curves to the experimental data,  $C^2S_\alpha = \frac{\sigma_{exp}}{\sigma_{DW} \cdot C^2S_\alpha^{7Li}}$ . The  $\alpha+t$  overlap spectroscopic factor  $C^2S_\alpha^{7Li} = 1$  [12]. With the  $C^2S_\alpha$  the partial  $\alpha$ -widths ( $\Gamma_\alpha$ ) were evaluated following Ref. [13] at the interaction radius  $r = 7.5$  fm where the  $\alpha+^{17}\text{O}$  wave function reaches an asymptotic behavior [14].

The normalized DWBA curves in Fig. 2 were obtained with  $\alpha+^{17}\text{O}$  Woods-Saxon parameters  $r_0 = 1.3$  fm and  $a = 0.70$  fm [15]. The optical potential parameters are given in [9]. Since the states considered in the present work are all unbound, the radial form factor was calculated using the weakly-bound approximation prescription [16, 17].

The good agreement between the DWBA calculations and the measured differential cross-sections gives strong evidence of the direct nature of the ( $^7\text{Li},t$ ) reaction populating most of the levels.

Given that the spin of  $^{17}\text{O}$  is  $5/2^+$ , we checked that higher  $\alpha$  orbital angular momenta, ( $\ell_\alpha$ ), do not contribute significantly [9].

The experimental differential cross-section of the 8.146/8.155/8.160-MeV triplet is fitted using a combination of two  $\ell_\alpha=2$  components, associated to the 8.146-MeV  $J^\pi = 3/2^+$  and the 8.155-MeV,  $J^\pi = (9/2^+)$  states and an  $\ell_\alpha=0$  component for the 8.160-MeV,  $J^\pi = 5/2^+$  state. The  $C^2S_\alpha$  of the 8.146 and 8.160 MeV states were derived using their corresponding  $\alpha$ -widths measured in [18] while that of the 8.155-MeV state was deduced here from the fit of the three combined DWBA calculations to the extracted data. Since the spin-parity of the 8.155-MeV state may also be  $9/2^-$  [4], a further fit was performed taking this into account with  $\ell_\alpha=3$ . This led to an  $\alpha$ -width inconsistent with the  $^{17}\text{O}(\alpha,\gamma)^{21}\text{Ne}$  resonance strength [19] and a  $J^\pi = 9/2^-$  assignment is not supported.

For the 7.980/7.982-MeV doublet, the data were fitted by a combination of an  $\ell_\alpha=1$  (7.980-MeV,  $3/2^-$ ) component for which the  $C^2S_\alpha$  was deduced using the  $\omega\gamma_{(\alpha,n)}$  resonance strength of [20, 21], the  $\Gamma_n$  from Ref. [5] and the  $\Gamma_\gamma$  from Ref. [22], and an  $\ell_\alpha=2$  (7.982-MeV,  $(7/2^+)$ ) component for which the  $C^2S_\alpha$  was deduced from the fit to the present data. A fit using the other possible [ $J^\pi = 11/2^+$ ,  $\ell_\alpha=4$ ] assignment for the  $E_x = 7.982$  MeV state [4] was also performed. This, too, was inconsistent with the measured resonance strength [19].

Concerning the 7.74- and 7.82-MeV states, for which the  $J^\pi$  are unknown, the experimental differential cross-sections were fitted considering different  $\ell_\alpha$ , from 0 to 4. The  $E_x = 7.74$ -MeV state data do not discriminate between the different assignments. For the 7.82-MeV state,  $\chi^2$ -minimization favours  $\ell_\alpha=0-2$ . However, with  $\ell_\alpha=0$ , the obtained  $C^2S_\alpha$  is unreasonably large (0.61) for such a high excitation energy considering that the  $\alpha$ -strength is already shared among the three  $5/2^+$  low lying states which  $C^2S_\alpha$  are found large [23].

The obtained  $C^2S_\alpha$  for each populated state in  $^{21}\text{Ne}$  are displayed in Table I together with their deduced  $\alpha$  partial widths. The  $E_x=7.74$  MeV and  $E_x=7.82$  MeV states are reported for  $\ell_\alpha=0$  and  $\ell_\alpha=1$ , respectively. These are the values used for the calculation of the reaction rates displayed in Fig. 3. The choice of  $\ell_\alpha=0$  for the 7.74-MeV ensures a consistent comparison with the previous ones.

TABLE I. Spectroscopic factors and  $\alpha$ -widths from present work (unless otherwise specified) for relevant  $^{21}\text{Ne}$  states. The tabulated excitation energies and their uncertainties come from Ref. [5] except the  $E_x = 8.155$ -,  $8.009$ -,  $7.980$ - and  $7.74$ -MeV states which come from Ref. [4].

$E_x$ (keV)	$E_r^{c.m.}$ (keV)	$J^\pi$	$\ell_\alpha$	$C^2S_\alpha^a$	$\Gamma_\alpha^b$ (meV)
7420.4(15)	72.5(15)	$11/2^-$	3	0.110(5)	$258(88) \times 10^{-34}$
7470(2)	122(2)	$3/2^-$	1	0.029(19)	$101(75) \times 10^{-22}$
7559.1(15)	211.2(15)	$(5/2^+)$	0	0.173(21)	$328(120) \times 10^{-13}$
7602.0(15)	254.1(15)	$7/2^-$	1	0.066(10)	$150(55) \times 10^{-11}$
7619.9(10)	272.0(10)	$3/2^-$	1	0.042(15)	$619(300) \times 10^{-11}$
7655.7(22)	307.8(22)	$7/2^+$	2	0.0200(74)	$176(88) \times 10^{-10}$
7740(10)	392(10)	$(5/2^+)$	0	0.155(36)	$343(140) \times 10^{-6}$
7820.1(15)	472.2(15)	$(7/2^-)$	1	0.260(39) <sup>c</sup>	$157(59) \times 10^{-4c}$
7960(2)	612(2)	$11/2^-$	3	0.0110(15)	$300(111) \times 10^{-5}$
7980(10)	632(10)	$3/2^-$	1	0.03 <sup>d</sup>	$410(52) \times 10^{-3d}$
7982.1(7)	634.2(7)	$(7/2^+)$	2	0.0050(12)	$191(76) \times 10^{-4}$
8009(10)	661(10)	$1/2^-$	3	$\leq 0.001^e$	$\leq 6.50 \times 10^{-4e}$
8069(1)	721(1)	$3/2^+$	2	0.0470(47)	1.54(54)
8146(2)	798(2)	$3/2^+$	2	0.34 <sup>f</sup>	54.7(55) <sup>f</sup>
8155.0(10)	807(1)	$(9/2^+)$	2	0.1500(165)	28.4(102)
8160(2)	812(2)	$5/2^+$	0	0.012 <sup>f</sup>	16.0(16) <sup>f</sup>

<sup>a</sup> Uncertainties are statistical. See text for systematic uncertainties

<sup>b</sup> Uncertainties are the quadratic sum of the statistical and the DWBA uncertainties (see text for details).

<sup>c</sup> For  $\ell_\alpha=0$ ,  $J^\pi = 5/2^+$ ,  $C^2S_\alpha = 0.610(9)$  and  $\Gamma_\alpha = 683 \times 10^{-4}$  meV. for  $\ell_\alpha=2$ ,  $J^\pi = 3/2^+$ ,  $C^2S_\alpha = 0.310(5)$  and  $\Gamma_\alpha = 465 \times 10^{-5}$  meV.

<sup>d</sup>  $C^2S_\alpha$  is deduced from the  $(\alpha,n)$  resonant strength [20, 21].

<sup>e</sup> An upper limit for  $C^2S_\alpha$  was deduced from the non-observation of this state.

<sup>f</sup>  $C^2S_\alpha$  are derived from the  $\Gamma_\alpha$  of Ref. [18].

The uncertainties on the  $C^2S_\alpha$  were evaluated by investigating different entrance [24–27] and exit [28, 29] optical potentials as well as different geometry for the  $\alpha+^{17}\text{O}$  interaction potential [15]; they were found to be of about 24% each. Nevertheless the uncertainty on the  $\Gamma_\alpha$  due to the well geometry was less than 5% due to compensation between  $C^2S_\alpha$  and the radial part of the  $\alpha+^{17}\text{O}$  wave function. The number of nodes  $N$  (5 or 6 including the origin) was found to have a limited impact on the  $\alpha$ -width ( $\leq 6\%$ ) (see [16]) while on  $C^2S_\alpha$  it is about 25%. The total uncertainty on  $\Gamma_\alpha$  due to the

DWBA model is about 35%.

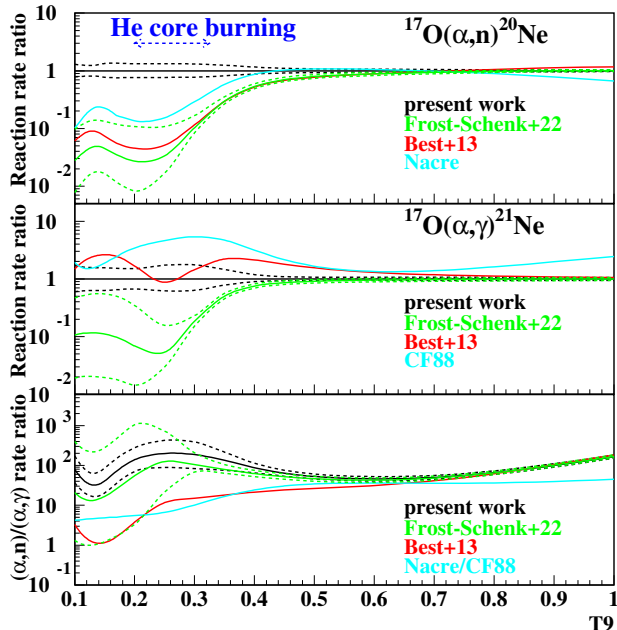


FIG. 3. (Color online) The  $^{17}\text{O}(\alpha, n)^{20}\text{Ne}$  (top) and  $^{17}\text{O}(\alpha, \gamma)^{21}\text{Ne}$  (middle) reaction rates from the present work (black lines) and those of [5] (green), [18] (red), Nacre [30] and CF88 [31] (turquoise) normalized to our recommended rate. See text for details. The indicated blue range of 0.2-0.3 GK corresponds to He-core burning in massive stars. (bottom) The  $^{17}\text{O}(\alpha, n)^{20}\text{Ne}$  to  $^{17}\text{O}(\alpha, \gamma)^{21}\text{Ne}$  reaction rates ratio. The solid black line displays the ratio of our recommended rates and the dashed black lines display the ratios of the upper (lower)  $^{17}\text{O}(\alpha, n)^{20}\text{Ne}$  rate to the lower (upper)  $^{17}\text{O}(\alpha, \gamma)^{21}\text{Ne}$  reaction rates.

$^{17}\text{O}(\alpha, n)^{20}\text{Ne}$  and  $^{17}\text{O}(\alpha, \gamma)^{21}\text{Ne}$  reaction rates were calculated using the Monte-Carlo code RATESMC [32]. A Gaussian probability density function is assumed for the resonance energies (Table I) and a log-normal distribution for the partial widths. The resonance parameters of the excited states from 7.420 MeV to 8.160 MeV used in the calculations are given in [9]. For the resonant states of astrophysical interest at  $E_x = 8.155$  MeV and below  $E_x = 8.069$  MeV except the 7.980-MeV, the  $\alpha$ -widths and their associated uncertainties considered in the calculations are those deduced experimentally for the first time in the present work (see Table I).

For the neutron partial widths, the experimental values determined in Ref. [5], using the  $^{20}\text{Ne}(d, p)^{21}\text{Ne}$  transfer reaction, were used, except for the 7.820-MeV state for which a neutron width of  $\Gamma_n = 29(3)$  eV was calculated using the  $C^2S_n$  deduced from the analysis of the 7.820-MeV angular distributions of Ref. [5] also consistent with a neutron angular momentum  $l_n = 3$ . For the  $\gamma$ -partial widths, the mean value 0.20(14) eV deduced from the mean measured lifetime [22] was considered as in Ref.

[5]. For states where the neutron-width is unknown, the assumption of Ref. [18] for the ratio of the  $\gamma$ -width to the neutron width was adopted.

For the states at and above  $E_x = 8.069$  MeV except the 8.155-MeV, the  $\Gamma_\alpha$  and the  $\Gamma_n$  coming from the  $(\alpha, n)$  measurements of Ref. [18] were considered. Since no uncertainties were associated to the given values, an arbitrary 10% precision was assumed for all of them. For the  $^{17}\text{O}(\alpha, \gamma)^{21}\text{Ne}$  rate calculation, the recent adopted  $(\alpha, \gamma)$  resonance strengths given in Ref. [19] for the  $E_r^{c.m.} = 634.2$ -, 721- and 807-keV resonances were used.

To properly account for the uncertain  $\ell_\alpha$  values for the 7.740- and 7.820-MeV states, the rates have been calculated separately for two extreme cases considering the largest/smallest contribution for each state [9]. This prevents the median rate from falling between the two likely rate values, see Ref. [33] for an example of this effect.

The calculated  $^{17}\text{O}(\alpha, n)^{20}\text{Ne}$  and  $^{17}\text{O}(\alpha, \gamma)^{21}\text{Ne}$  reaction rates from Refs. [5, 18, 30, 31] normalized to our recommended rates (corresponding to the 50th percentile of the cumulative rate distribution) given numerically in [9] are shown in Fig. 3 together with our evaluated high and low rates which represent a coverage probability of 68%. At the temperatures of interest (0.2 – 0.3 GK), our  $(\alpha, n)$  recommended reaction rate is higher by a factor of about 6, 20 and 30 in comparison to the rates of Refs. [30], [18] and [5], respectively. This is due to the major improvement brought by the present work: the first experimental determination of the  $C^2S_\alpha$  and  $\alpha$ -widths of the astrophysically important states. In Ref. [18] the  $\alpha$ -widths for all the states below 8.069 MeV were evaluated assuming a  $C^2S_\alpha$  of 0.01 and in Ref. [5] were sampled from a Porter-Thomas distribution assuming a dimensionless reduced  $\alpha$ -width of 0.01.

For the  $(\alpha, \gamma)$  rate, our recommended rate in the region of interest is comparable within a factor two, 18 times larger and five times smaller than the rates of Ref. [18], Ref. [5] and [31], respectively.

The ratio of the present  $^{17}\text{O}(\alpha, n)^{20}\text{Ne}$  to  $^{17}\text{O}(\alpha, \gamma)^{21}\text{Ne}$  reaction rates is also shown in Fig. 3 together with those of Refs. [5], [18] and [30] to [31] rate ratio. The present evaluated reaction rate ratio is found to be larger by a factor of about 2 and 20 than those of Refs. [5] and [18], respectively, and by a factor of about 30 than the NACRE/CF88 ratio at the temperatures between 0.2 to 0.3 GK. The uncertainties on the  $^{17}\text{O}(\alpha, n)^{20}\text{Ne}$  and  $^{17}\text{O}(\alpha, \gamma)^{21}\text{Ne}$  rates of about 32% and 77%, respectively, were drastically reduced in the region of interest in comparison to Ref. [5] thanks to the present experimental determination of the  $\alpha$ -widths of  $^{21}\text{Ne}$  states.

From the fractional contribution of each resonance to the rates at each temperature [9], the dominant contributions at 0.2-0.3 GK come from the  $E_r^{c.m.} = 392$ - and

472.2-keV resonances for  $(\alpha, n)$  and those at  $E_r^{c.m.}=308$  and 472.2 keV for  $(\alpha, \gamma)$ .

Given the unconstrained  $\ell_\alpha$  value for the 7.74-MeV ( $E_r^{c.m.} = 392$  keV) state and the three possible values for the 7.82-MeV ( $E_r^{c.m.}=472.2$  keV) state, the  $J^\pi$  of both states need to be constrained. Reaction rate calculations with  $\ell_\alpha=2$  for the 7.82-MeV state and no contribution from the 7.74-MeV state, the smallest contribution case based on the current study, were also performed and reported in Table IV and V of [9]. Even in this extreme case the  $(\alpha, n)/(\alpha, \gamma)$  reaction rate ratio is twenty (ten) times larger than NACRE/CF88 (Best [18]).

The impact of the new  $^{17}\text{O}(\alpha, n)^{20}\text{Ne}$  and  $^{17}\text{O}(\alpha, \gamma)^{21}\text{Ne}$  rates on the  $s$ -process nucleosynthesis in a  $25 M_\odot$  metal-poor rotating massive star was investigated with a one-zone nucleosynthesis calculation mimicking rotation-induced mixing during core He burning [5, 34]. A large enhancement ( $>1.5$  dex) of  $s$ -elements between Zr ( $Z=40$ ) and Nd ( $Z=60$ ) is found with the present rates calculated with  $\ell_\alpha=0$  and  $\ell_\alpha=1$  for the 7.74-MeV and 7.82-MeV states, respectively (red curve) compared to Ref. [18] (see Fig. 4).

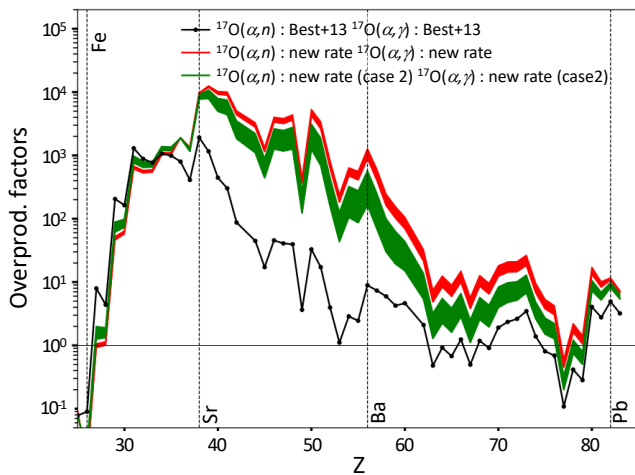


FIG. 4. (Color online) Overproduction factors in the  $s$ -process for a metal-poor rotating massive star of  $25M_\odot$  at a metallicity of  $Z=0.001$ . The results using the present rates are in red and green (see text for details), those using Ref. [18] are in black. The thickness of the red and green curves represent the uncertainties due to those of our recommended rates.

For Ba, the enhancement is even larger: 2 dex. This enhancement is still much larger than that of Ref. [18] even with the smallest expected rate (green curve) calculated with  $\ell_\alpha=2$  for the 7.82-MeV state and no contribution of the 7.74 MeV.

This boosted  $s$ -process is in line with the observation of an enhanced  $s$ -process in globular cluster NGC6522 [35] and in the CEMP-s(Carbon-Enhanced Metal-Poor) stars [36].

In this Letter, we reported the first experimental deter-

mination of the  $\alpha$ -spectroscopic factors and  $\alpha$ -widths of  $^{21}\text{Ne}$  states within the energy range for He-core burning in massive stars. The uncertainties of the  $^{17}\text{O}(\alpha, n)^{20}\text{Ne}$  and  $^{17}\text{O}(\alpha, \gamma)^{21}\text{Ne}$  reaction rates were improved by a factor more than three and their ratio is found to greatly exceed previous evaluations. This favors efficient recycling of neutrons and an enhancement of the weak  $s$ -process yields in the Zr-Nd region by more than 1.5 dex in low-metallicity rotating massive stars.

The authors would like to thank the beam operators at the Maier-Leibnitz-Laboratorium and the INFN-LNS target laboratory for the high-quality beam and enriched targets they produced, respectively. FH would like to thank Alison Laird for the discussions on  $^{20}\text{Ne}(d, p)^{21}\text{Ne}$  results, Pierre Descouvemont for the fruitful discussions and BERRY ASSOCIATES INC company for providing us the enriched  $\text{WO}_3$  powder for free. PA thanks the trustees and staff of the Claude Leon Foundation for support in the form of a postdoctoral fellowship and Andreas Best for helpful comments on previous experimental studies of  $^{17}\text{O} + \alpha$ . RH acknowledges support from the World Premier International Research Centre Initiative (WPI Initiative, MEXT, Japan), STFC UK, the European Union’s Horizon 2020 research and innovation programme under grant agreement No 101008324 (ChETEC-INFRA) and the IReNA AccelNet Network of Networks, supported by the National Science Foundation under Grant No. OISE-1927130. This work was supported by the Fonds de la Recherche Scientifique-FNRS under Grant No IISN 4.4502.19.

\* fairouz.hammache@ijclab.in2p3.fr

† Present address: Cyclotron Institute and Department of Physics & Astronomy, Texas A&M University, College Station, Texas 77843, USA

- [1] F. Rizzuti, G. Cescutti, F. Matteucci, A. Chieffi, R. Hirschi, M. Limongi, and A. Saro, MNRAS **502**, 2495 (2021), arXiv:2101.05345 [astro-ph.GA].
- [2] N. Nishimura, R. Hirschi, T. Rauscher, A. St. J. Murphy, and G. Cescutti, MNRAS **469**, 1752 (2017), arXiv:1701.00489 [astro-ph.SR].
- [3] A. Choplin, R. Hirschi, G. Meynet, S. Ekström, C. Chiappini, and A. Laird, Astron. Astrophys. **618**, A133 (2018), arXiv:1807.06974 [astro-ph.SR].
- [4] “ENSDF, NNDC online data service, ENSDF database,” <http://www.nndc.bnl.gov/ensdf/> (2015).
- [5] J. Frost-Schenk, P. Adsley, A. M. Laird, R. Longland, C. Angus, C. Barton, A. Choplin, C. A. Diget, R. Hirschi, C. Marshall, F. Portillo Chaves, and K. Setoodehnia, MNRAS **514**, 2650 (2022), arXiv:2206.04167 [nucl-ex].
- [6] M. Löffler, H. Scheerer, and H. Vonach, Nucl. Instrum. Methods **111**, 1 (1973).
- [7] C. O. Bacri, C. Bachelet, C. Baumier, J. Bourçois, L. Delbecq, D. Ledu, N. Pauwels, S. Picard, S. Renouf, and C. Tanguy, Nucl. Instrum. Methods Phys. Res. B **406**,



- 48 (2017).
- [8] H.-F. Wirth, H. Angerer, T. von Egidy, Y. Eisermann, G. Graw, and R. Hertenberger, *Jahresbericht BL 2000*, 71 (2001).
- [9] See Supplemental Material [url] for Sec.1 which includes Ref. [10],  $^{22}\text{Ne}$  contamination from  $^{18}\text{O}(^7\text{Li,t})^{22}\text{Ne}$  reaction; Sec.2, Differential cross-sections of the 7.559-, 7.602- and 7.620- MeV  $^{21}\text{Ne}$  states; Sec.3, optical potential parameters used for the DWBA analysis which includes Refs. [25, 26, 29]; Sec.4, DWBA calculations with higher orbital angular momenta ; Sec.5, the tabulated median, low and high reaction rates obtained in the present work and the resonance parameters used; Sec.6, the plots of the fractional contributions of  $^{21}\text{Ne}$  resonant states to the  $^{17}\text{O}(\alpha,n)^{20}\text{Ne}$  and  $^{17}\text{O}(\alpha,\gamma)^{21}\text{Ne}$  rates.
- [10] U. Giesen, C. Browne, J. Görres, J. Ross, M. Wiescher, R. Azuma, J. King, J. Vise, and M. Buckby, *Nuclear Physics A* **567**, 146 (1994).
- [11] I. J. Thompson, *Comput. Phys. Rep.* **7**, 167 (1988).
- [12] M. G. Pellegriti, F. Hammache, P. Roussel, L. Audouin, D. Beaumel, P. Descouvemont, S. Fortier, L. Gaudefroy, J. Kiener, A. Lefebvre-Schuhl, M. Stanoiu, V. Tatischeff, and M. Vilmay, *Phys. Rev. C* **77**, 042801(R) (2008).
- [13] C. Iliadis, *Nuclear Physics of Stars* (Wiley-VCH, 2008).
- [14] N. de Séréville, A. Meyer, F. Hammache, A. M. Laird, and M. Pignatari, in *EPJ Web Conf.*, Vol. 165 (2018) p. 01022.
- [15] K. I. Kubo and M. Hirata, *Nucl. Phys. A* **187**, 186 (1972).
- [16] F. Hammache and N. de Séréville, *Frontiers in Physics* **8**, 630 (2021), arXiv:2107.13228 [nucl-ex].
- [17] A. Meyer, N. de Séréville, A. M. Laird, F. Hammache, R. Longland, T. Lawson, M. Pignatari, L. Audouin, D. Beaumel, S. Fortier, J. Kiener, A. Lefebvre-Schuhl, M. G. Pellegriti, M. Stanoiu, and V. Tatischeff, *Phys. Rev. C* **102**, 035803 (2020), arXiv:2006.13589 [nucl-ex].
- [18] A. Best, M. Beard, J. Görres, M. Couder, R. deBoer, S. Falahat, R. T. Güray, A. Kontos, K. L. Kratz, P. J. LeBlanc, Q. Li, S. O'Brien, N. Özkan, M. Pignatari, K. Sonnabend, R. Talwar, W. Tan, E. Uberseder, and M. Wiescher, *Phys. Rev. C* **87**, 045805 (2013), arXiv:1304.6443 [nucl-ex].
- [19] M. Williams, A. M. Laird, A. Choplin, P. Adsley, B. Davids, U. Greife, K. Hudson, D. Hutcheon, A. Lennarz, and C. Ruiz, *Phys. Rev. C* **105**, 065805 (2022), arXiv:2206.06016 [nucl-ex].
- [20] A. Denker, H. W. Drotleff, M. Große, J. W. Hammer, H. Knee, R. Kunz, A. Mayer, R. Seidel, and G. Wolf, in *Nuclear Astrophysics* (1993) p. 123.
- [21] A. Denker, Thesis, Universität Stuttgart (1994).
- [22] C. Rolfs, H. P. Trautvetter, E. Kuhlmann, and F. Riess, *Nucl. Phys. A* **189**, 641 (1972).
- [23] N. Anantaraman, H. E. Gove, J. Töke, and H. T. Fortune, *Physics Letters B* **74**, 199 (1978).
- [24] P. Schumacher, N. Ueta, H. H. Duhm, K.-I. Kubo, and W. J. Klages, *Nucl. Phys. A* **212**, 573 (1973).
- [25] K. I. Kubo, F. Nemoto, and H. Bando, *Nucl. Phys. A* **224**, 573 (1974).
- [26] V. I. Chuev, V. Davidov, A. Novatskii, S. B. Ogloblin, S. B. Sakuta, and S. D. N, in *Journal de Physique*, Colloque 6, suppl 11-12, Vol. Tome 32 (1971) pp. c6-157, c6-161.
- [27] K. Bethge, C. M. Fou, and R. W. Zurmühle, *Nucl. Phys. A* **123**, 521 (1969).
- [28] C. M. Perey and F. G. Perey, *Atomic Data and Nuclear Data Tables* **17**, 1 (1976).
- [29] J. D. Garrett and O. Hansen, *Nucl. Phys. A* **212**, 600 (1973).
- [30] C. Angulo, M. Arnould, M. Rayet, P. Descouvemont, D. Baye, C. Leclercq-Willain, A. Coc, S. Barhoumi, P. Aguer, C. Rolfs, R. Kunz, J. W. Hammer, A. Mayer, T. Paradellis, S. Kossionides, C. Chronidou, K. Spyrou, S. degl'Innocenti, G. Fiorentini, B. Ricci, S. Zavatarelli, C. Providencia, H. Wolters, J. Soares, C. Grama, J. Rahighi, A. Shotter, and M. Lamehi Rachti, *Nucl. Phys. A* **656**, 3 (1999).
- [31] G. R. Caughlan and W. A. Fowler, *Atomic Data and Nuclear Data Tables* **40**, 283 (1988).
- [32] R. Longland, C. Iliadis, A. E. Champagne, J. R. Newton, C. Ugalde, A. Coc, and R. Fitzgerald, *Nucl. Phys. A* **841**, 1 (2010), arXiv:1004.4136 [astro-ph.SR].
- [33] D. S. Harrouz, N. de Séréville, P. Adsley, F. Hammache, R. Longland, B. Bastin, T. Faestermann, R. Hertenberger, M. La Cognata, L. Lamia, A. Meyer, S. Palmerini, R. G. Pizzone, S. Romano, A. Tumino, and H.-F. Wirth, *Phys. Rev. C* **105**, 015805 (2022).
- [34] A. Choplin, A. Maeder, G. Meynet, and C. Chiappini, *Astron. Astrophys.* **593**, A36 (2016), arXiv:1606.02752 [astro-ph.SR].
- [35] B. Barbuy, M. Zoccali, S. Ortolani, V. Hill, D. Minniti, E. Bica, A. Renzini, and A. Gómez, *Astron. Astrophys.* **507**, 405 (2009), arXiv:0908.3603 [astro-ph.GA].
- [36] T. C. Beers and N. Christlieb, *Annual Review of Astronomy and Astrophysics* **43**, 531 (2005).